Modeling Regulation of Cardiac K_{ATP} and L-type Ca^{2+} Currents by ATP, ADP, and Mg^{2+}

Anushka Michailova, Jeffrey Saucerman, Mary Ellen Belik, and Andrew D. McCulloch
Department of Bioengineering, University of California San Diego, La Jolla, California

ABSTRACT Changes in cytosolic free Mg^{2+} and adenosine nucleotide phosphates affect cardiac excitability and contractility. To investigate how modulation by Mg^{2+}, ATP, and ADP of K_{ATP} and L-type Ca^{2+} channels influences excitation-contraction coupling, we incorporated equations for intracellular ATP and MgADP regulation of the K_{ATP} current and MgATP regulation of the L-type Ca^{2+} current in an ionic-metabolic model of the canine ventricular myocyte. The new model: 1), quantitatively reproduces a dose-response relationship for the effects of changes in ATP on K_{ATP} current, 2), simulates effects of ADP in modulating ATP sensitivity of K_{ATP} channel, 3), predicts activation of Ca^{2+} current during rapid increase in MgATP, and 4), demonstrates that decreased ATP/ADP ratio with normal total Mg^{2+} or increased free Mg^{2+} with normal ATP and ADP activate K_{ATP} current, shorten action potential, and alter ionic currents and intracellular Ca^{2+} signals. The model predictions are in agreement with experimental data measured under normal and a variety of pathological conditions.

INTRODUCTION

Pathological changes of intracellular free and bound Mg^{2+}, ATP, and ADP concentrations occur during ischemia, and reperfusion and the concentrations of these metabolites have been shown to affect the availability and activity of ATP-sensitive K^+ and L-type Ca^{2+} channels and consequently cell excitability and contractility (Noma, 1983; Agus et al., 1989; Carmeliet, 1999; Bers, 2001; Michailova and McCulloch, 2001).

The ATP-sensitive K^+ channels were first discovered by Noma (1983) in the plasma sarcolemmal membrane of cardiac myocytes. Normally, K_{ATP} channel activity is inhibited by intracellular free ATP. When ATP is depleted, sarcolemmal K_{ATP} channels open to hyperpolarize the cell. Thus, K_{ATP} channels couple cell metabolism to its electrical activity. These channels are also regulated by a variety of other intracellular and extracellular factors, including MgADP, MgATP, pH, G-proteins, adenosine, and extracellular ATP (Ashcroft and Ashcroft, 1990; Nichols and Lederer, 1991). Experimental data suggest that the sarcolemmal K_{ATP} channel consists of two types of subunits—pore-forming K^+-channel subunits (Kir6) and sulphonylurea receptor subunits (SUR) (Inagaki et al., 1995). During the past few years, the cloning of these subunits has led to significant advances in our understanding of K_{ATP} channel structure-function relations. Both subunits are required to form a functional K_{ATP} channel, coassembling in an obligate 4:4 stoichiometry to form an octameric channel (Clement et al., 1997; Shyng and Nichols, 1997). Two different Kir6 subunit genes have been described, Kir6.1 and Kir6.2 (Inagaki et al., 1995; Sakura et al., 1995). Two closely related genes encoding the sulphonylurea receptors, SUR1 and SUR2, have been also cloned (Aguilar-Bryan et al., 1995; Inagaki et al., 1996). The various Kir and SUR subunits ''mix and match'' to form K_{ATP} channels with different pharmacological and nucleotide sensitivities. Comparison of the properties of cloned and wild-type K_{ATP} channels suggests that cardiac K_{ATP} channel is composed from Kir6.2 and SUR2A (Inagaki et al., 1995, 1996; Sakura et al., 1995; Aguilar-Bryan et al., 1995). A key question has been which properties of the K_{ATP} channel are intrinsic to Kir and which are endowed by SUR. The primary site at which intracellular free ATP acts to cause K_{ATP} channel inhibition appears to lie on Kir6.2 (Nichols and Lederer, 1991; Ashcroft and Gribble, 1998; Ribalet et al., 2003), whereas SUR2A is the principal target for pharmacological agents (Aguilar-Bryan et al., 1995; Inagaki et al., 1996). SUR2A also mediates the stimulatory effects of intracellular MgADP and enhances channel open probability (Nichols et al., 1996c; Tucker et al., 1997; Trapp et al., 1997; Proks and Ashcroft, 1997).

Several attempts have been made to integrate a simple Hill-type formulation for the ATP regulation of K_{ATP} channel current ($I_{K(ATP)}$) into existing electrophysiological cell models, assuming channel availability as a function of absolute ATP concentration ($f_{K(ATP)} \sim [ATP]_{tot}$), (Nichols et al., 1991a; Shaw and Rudy, 1994, 1997; Ferrero et al., 1996; Rodriguez et al., 2002; Matsuoka et al., 2003; Fridlyand et al., 2003). This was mainly because these ionic models did not calculate intracellular free ATP, MgADP, and MgADP, which are known to regulate the ligand-gated channel activity.

Noma and Shibasaki (1985) first demonstrated the ATP dependence of the L-type Ca^{2+} current, which was independent of membrane potential and protein phosphorylation.

Submitted May 25, 2004, and accepted for publication November 19, 2004.

Address reprint requests to Dr. Anushka Michailova, Dept. of Bioengineering, University of California San Diego, La Jolla, CA 92093-0412. E-mail: amihaylo@bioeng.ucsd.edu.

Abbreviations used: ATP, adenosine triphosphate; ADP, adenosine diphosphate; AP, action potential; EC coupling, excitation-contraction coupling; RyR, ryanodine receptor; SERCA2a, SR Ca^{2+} ATPase; SR, sarcoplasmic reticulum; TnC, troponin C.

0006-3495/05/03/2234/16 $2.00

doi: 10.1529/biophysj.104.046284

Later, using flash photolysis of caged Mg^{2+} or ATP, it was found that the rapid changes in intracellular MgATP, rather than free ATP, may increase the whole-cell I_{Ca} current without significantly affecting gating kinetics (O'Rourke et al., 1992). The rate of increase in whole-cell I_{Ca} current (O'Rourke et al., 1992) and probability distributions from inside-out patches (Yazawa et al., 1997) suggested that the MgATP regulation of I_{Ca} is the result of an increase in channel availability (f_{Ca}). To simulate the effects of changes in intracellular ATP level on L-type Ca^{2+} current, Shaw and Rudy (1997) and Matsuoka et al. (2003) used a Hill-type approximation, assuming $f_{Ca} \sim [ATP]_{tot}$.

Therefore, the goals of this study were: 1), to formulate a new model for cardiac K_{ATP} current regulation by intracellular free ATP and MgADP that takes into account the octameric channel stoichiometry; 2), to formulate a new reduced-order model of the L-type Ca^{2+} channel and to incorporate the direct regulation of the L-type Ca^{2+} current by MgATP; 3), to integrate these models into our whole cell ventricular model (Michailova and McCulloch, 2001; Michailova et al., 2004b); and 4), to investigate how changes in intracellular free Mg^{2+} and adenine nucleotide phosphate levels modulate K_{ATP} current, Ca^{2+} current, and the integrated process of excitation-contraction coupling.

The new model reproduces experimental data on the ATP dependence of K_{ATP} channel activity in the presence of normal ADP and Mg^{2+} and the effects of stimulated K_{ATP} current on cell excitability and contractility (Nichols et al., 1991a). The model is also able to simulate and predict: a), the effects of ADP in modulating ATP sensitivity of the K_{ATP} channel, b), the activation of L-type Ca^{2+} current during rapid increase in intracellular MgATP concentration, and c), the effects of ATP in the absence of MgADP or of MgADP in the absence of ATP on macroscopic K_{ATP} current during a single beat. A reduction in total ATP/ADP ratio with normal $[Mg^{2+}]_{tot}$ or an increase of free Mg^{2+} with total ATP and ADP at normal levels increased $I_{K(ATP)}$, shortened action potential duration, and affected ionic currents and intracellular Ca^{2+} levels. Variations in absolute ATP and ADP levels with total Mg^{2+} and ATP/ADP ratio unchanged affected K_{ATP} and L-type channel activity and cardiac EC coupling. Preliminary results of this work have been presented to the Biophysical Society in abstract form (Michailova et al., 2004a).

MATHEMATICAL MODEL

Ionic-metabolic model

The whole-cell ionic-metabolic model is described in Michailova and McCulloch (2001). In that article, we extended the ionic model of the ventricular myocyte by Winslow et al. (1999) to examine the role of ATP and ADP as Ca^{2+} and Mg^{2+} buffers, transporters, and ion current regulators. The model cell has three spaces: subspace, myoplasm, and sarcoplasmic reticulum (see Fig. 1). Adenine nucleotides (ATP, ADP) and Mg^{2+} react and diffuse within subspace and myoplasm and not in the sarcoplasmic reticulum. Because MgATP is the preferred substrate for a large number of intracellular enzymes, ATP-dependent transporters and channels (Carmeliet, 1999; Bers, 2001), we also assumed that myoplasmic MgATP ($[MgATP]_i$) regulates SR and sarcolemmal Ca^{2+}-ATPases (see Fig. 1). The equations describing Ca^{2+} and Mg^{2+} buffering and transport by ATP and ADP in the subspace and myoplasm and the modified Winslow et al. (1999) equations for SERCA2a pump flux, $I_{p(Ca)}$ current, and free subspace and myoplasmic Ca^{2+} concentrations are shown in Appendix I.

Because Na^+-K^+ pump function is strongly ATP dependent (Bers, 2001) we previously assumed I_{NaK} current to be proportional to $[MgATP]_i$ as well. However, our predicted I_{NaK} current during ischemia (3 mM $[ATP]_{tot}$ and 12 mM $[K^+]_o$) was not in agreement with experimental data (Kleber, 1983; Carmeliet, 1999). For this reason, we tested the model assuming that I_{NaK} is independent of $[MgATP]_i$. The new calculations demonstrated better agreement with experimental data (Kleber, 1983). Therefore, in our current whole-cell model the I_{NaK} current is not $[MgATP]_i$ dependent (see Fig. 1).

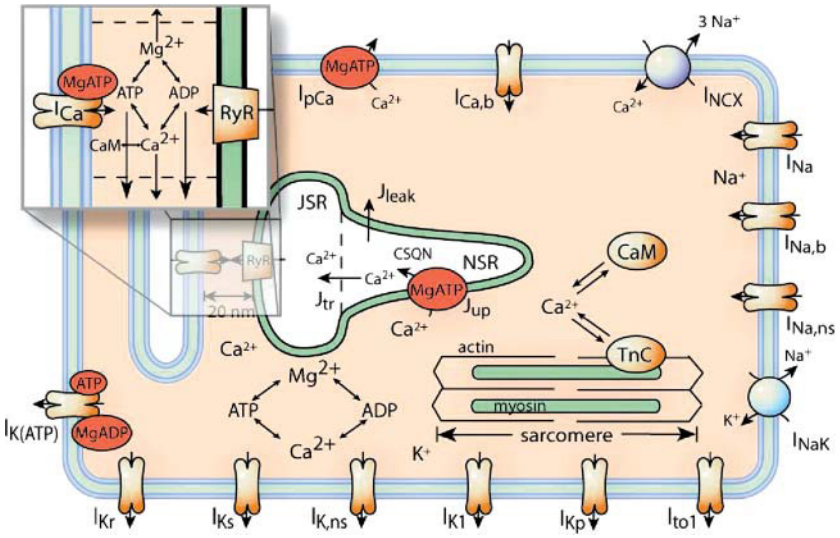

FIGURE 1 Schematic diagram illustrating Ca^{2+} and Mg^{2+} buffering and transport by ATP and ADP, adenine nucleotides regulation of ionic channels and pump, and electrophysiology in ventricular myocyte. See Appendix II for the notations of the parameters used throughout the study.

Modeling K_{ATP} channel availability

Taking into account experimental observations (Clement et al., 1997; Shyng and Nichols, 1997), we developed a model for the octameric cardiac K_{ATP} channel that contains four pore-forming subunits (Kir6.2) and four regulatory subunits (SUR2A) (Fig. 2 *A*). Binding of ATP to Kir6.2 and of MgADP to SUR2A is treated as instantaneous and the K_{ATP} channels were set on the plasma membrane (see Fig. 1). The general equation describing current density was as described in Shaw and Rudy (1997):

$$I_{K(ATP)} = g_{K(ATP)}(V - E_K) \quad (1)$$

$$g_{K(ATP)} = G_{K(ATP)} f_{K(ATP)} \left(\frac{[K^+]_o}{[K^+]_{o,normal}} \right)^{0.24} \quad (2)$$

The kinetics of ATP block of native cardiac K_{ATP} channels (Nichols et al., 1991b; Ashcroft and Gribble, 1998; Ribalet et al., 2003) suggest that there are four Kir6.2 sites that bind ATP independently with equal affinity, but that binding of only one molecule of ATP is sufficient to close the channel (Fig. 2 *A*). Thus, the fraction of sarcolemmal channels that are open because there is no ATP site occupied by ATP is:

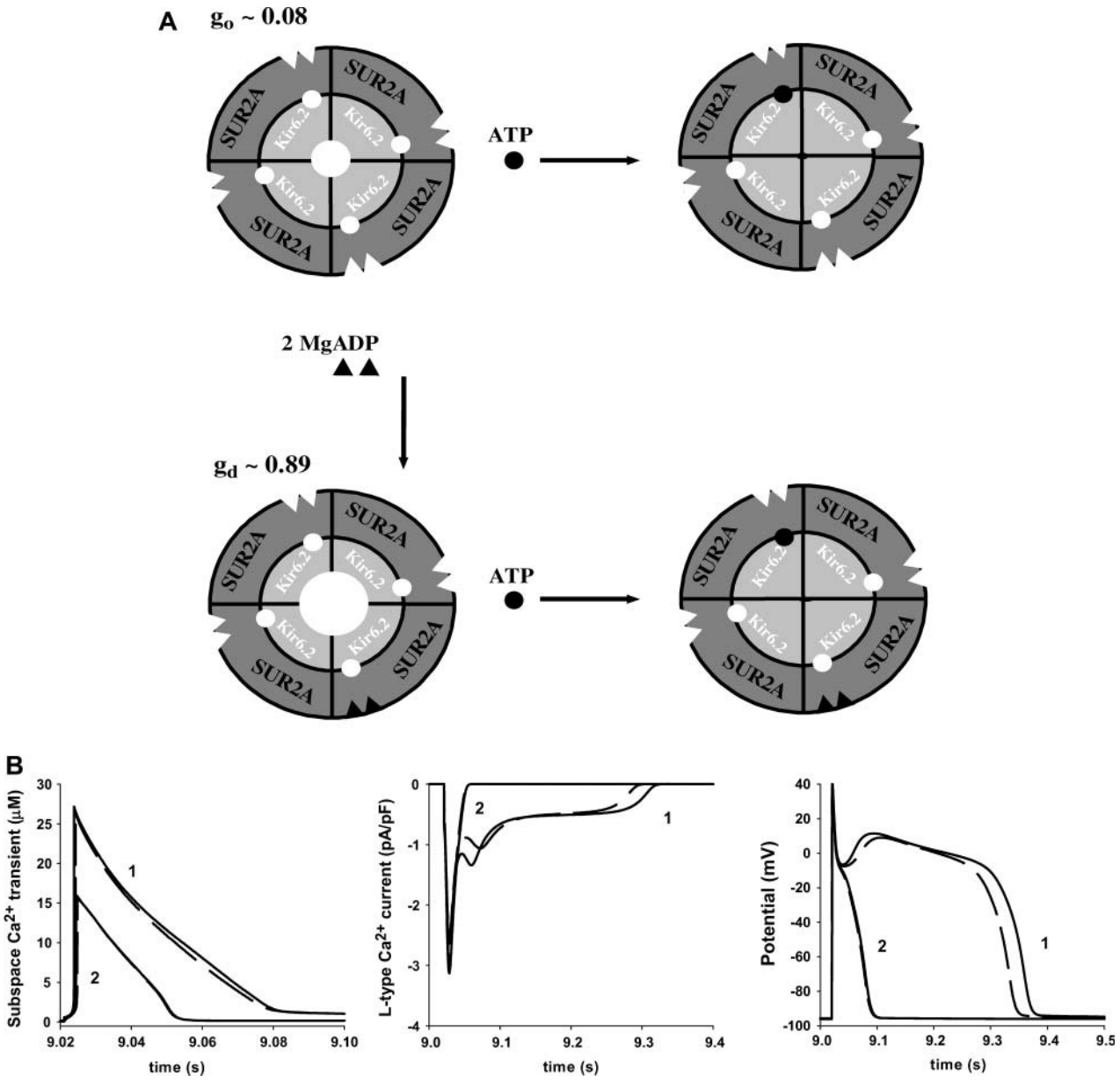

FIGURE 2 Schematic representation of Kir6.2 and SUR2A subunit stoichiometry in cardiac octameric K_{ATP} channel (*A*). It is assumed that the single ATP molecule (●) is sufficient to close the channel and that the binding of 2MgADP molecules (▲) to one SUR2A subunit increases the channel open probability. Panel *B* shows $[Ca^{2+}]_{ss}$, I_{Ca}, and action-potential time courses (9–10 s; 1-Hz frequency) generated with original ionic-metabolic model (*dashed lines*) and with reduced-order model of the L-type Ca^{2+} channel (*solid lines*). Normal condition (*1*) is 5 mM $[ATP]_{tot}$, 200 μM $[ADP]_{tot}$, 0.5 mM $[Mg^{2+}]_i$; metabolic inhibition (*2*) is 3 mM $[ATP]_{tot}$, 3 mM $[ADP]_{tot}$, 0.68 mM $[Mg^{2+}]_i$.

$$f_{ATP} = \left(1 - \frac{[ATP]_i}{[ATP]_i + k_{ATP}}\right)^4 \quad (3)$$

Experimental studies also suggest that channel activation by ADP requires the presence of Mg^{2+} (Nichols et al., 1996c; Gribble et al., 1997; Ueda et al., 1997; Ashcroft and Gribble, 1998). The simplest explanation for this could be that MgADP interacts with both SUR2A nucleotide binding domains (NBDs), that is, one MgADP molecule binds to each NBD, so that two molecules bind to each SUR2A subunit. It is not known whether the interaction of one or two MgADP molecules with only one of the four SUR2A subunits is sufficient to cause channel activation (Ashcroft and Gribble, 1998). Here we assume (see Fig. 2 *A*) that the simultaneous binding of two MgADP molecules to one SUR2A subunit is required to increase the channel open probability, i.e.:

$$f'_{MgADP} = \left(\frac{[MgADP]_i}{[MgADP]_i + k_{MgADP}}\right)^2 \quad (4)$$

Therefore, the fraction of sarcolemmal K_{ATP} channels that are closed because there are not two MgADP sites occupied by MgADP in one SUR2A subunit is:

$$c_{MgADP} = 1 - f'_{MgADP} \quad (5)$$

Because experimental studies suggest that there are four SUR2A subunits that bind MgADP independently and with equal affinity, the fraction of channels that are open because there are two MgADP molecules bound to only one SUR2A subunit is:

$$f_{MgADP} = 1 - (c_{MgADP})^4 \quad (6)$$

In this model, according to Hopkins et al. (1992), we also assume that when the channel has either no ATP or two MgADP molecules bound or two molecules MgADP bound, the channel is open with relative conductance of g_o and g_d, respectively (Fig. 2 *A*). This leads to the following expression for the dependence of the aggregate channel availability ($f_{K(ATP)}$) on adenine nucleotide concentrations when the two populations of K_{ATP} channels are open:

$$f_{K(ATP)} = g_o f_{ATP}(1 - f_{MgADP}) + g_d f_{ATP} f_{MgADP}, \quad (7)$$

or

$$f_{K(ATP)} = \left(1 - \frac{[ATP]_i}{[ATP]_i + k_{ATP}}\right)^4 \times \left\{ g_o \left(1 - \left(\frac{[MgADP]_i}{[MgADP]_i + k_{MgADP}}\right)^2\right)^4 + g_d \left(1 - \left(1 - \left(\frac{[MgADP]_i}{[MgADP]_i + k_{MgADP}}\right)^2\right)^4\right)\right\}$$

Finally, because many experimental studies suggest that a wide variety of intracellular and extracellular factors (MgATP, MgGDP, pH, G-proteins, phospholipids, extracellular ATP, adenosine) could additionally enhance channel open probability, here we also assumed that g_s ($g_s = 1 - g_o - g_d$) is the relative conductance accounting for this more complex ligand-gated channel regulation.

MgATP regulation in a reduced-order model of the L-type Ca^{2+} channel

A structurally motivated Markov model of the L-type Ca^{2+} channel parameterized with single-channel patch-clamp data (Jafri et al., 1998) has been used in a number of previous modeling studies (Rice et al., 1999; Winslow et al., 1999), including our past description of metabolism (Michailova and McCulloch, 2001). Here we sought to formulate a simplified model of the L-type Ca^{2+} channel, which retains the properties of the more detailed I_{Ca} Markov model yet reduces the complexity. To formulate the reduced-order I_{Ca} model, we began by assuming the structure and kinetics of the more detailed I_{Ca} Markov model (Jafri et al., 1998). From this starting point, several assumptions were made: 1), the four channel subunits gate independently of one another; 2), voltage-independent activation gating occurs independently of the voltage-dependent conformational changes in the subunits; 3), voltage-dependent inactivation occurs independently of activation and Ca^{2+}-dependent inactivation; 4), transitions between normal and Ca^{2+}-inactivated modes occur much more slowly than voltage-dependent gating within a mode. Assumptions 1 and 3 were made explicitly in the original I_{Ca} Markov model (Jafri et al., 1998). Assumptions 2 and 4 are supported both by timescale differences in the rate constants of the I_{Ca} Markov model (Jafri et al., 1998) and the single-channel data on which the I_{Ca} Markov model was based (Imredy and Yue, 1994). From these assumptions, a simplified set of equations can be derived with gating variables representing conditional probabilities for the channel state:

$$\frac{dv}{dt} = \alpha(1 - v) - \beta v \quad (8)$$

$$\frac{dw}{dt} = \alpha'(1 - w) - \beta' w \quad (9)$$

$$x = \frac{f}{f + g} \quad (10)$$

$$\frac{dy}{dt} = (y - y_\infty)/\tau_y \quad (11)$$

$$\frac{dz}{dt} = v_\omega(1 - z) - v_\gamma z \quad (12)$$

where $v_\omega = \omega \sum_{i=0}^{4} b^{-i} w^i (1-w)^{4-i}$ and $v_\gamma = \gamma[\sum_{i=0}^{4} a^i v^i (1-v)^{4-i} - a^4 v^4 x]$.

All parameters in Eqs. 8–12 remain identical to those used previously (Winslow et al., 1999; Michailova and McCulloch, 2001). Thus, using Eqs. 8–12 and the above assumptions, the probability of gating channel becomes:

$$P_{rom} = v^4 y z \frac{f}{f + g} \quad (13)$$

Further, taking into account experimental data (O'Rourke et al., 1992; Yazawa et al., 1997) and our whole-cell model topology (see Fig. 1) we modeled the relative Ca^{2+} channel availability (f_{Ca}) as a function of $[MgATP]_{ss}$ using the Hill-type equation.

$$f_{Ca} = \frac{1}{1 + \left(\frac{k_{MgATPss}}{[MgATP]_{ss}}\right)^{2.6}} \quad (14)$$

where $k_{MgATPss} = 1.4$ mM (from Shaw and Rudy, 1997).

Thus, the effect of MgATP regulation of the L-type Ca^{2+} channel current (I_{Ca}) and K^+ current through the channel ($I_{Ca,K}$) can be described by:

$$I_{Ca} = f_{Ca} \frac{\bar{P}_{Ca}}{C_{sc}} \frac{4VF^2}{RT} \frac{0.001 e^{\frac{2V}{RT}} - 0.34[Ca^{2+}]_o}{e^{\frac{2V}{RT}} - 1} P_{rom} \quad (15)$$

$$I_{Ca,K} = f_{Ca} \frac{P'_K}{C_{sc}} P_{rom} \quad (16)$$

where $\bar{P}_{Ca} = 3.594\,10^{-4}$ cm/s, $P'_k = 6.658\,10^{-7}$ cm/s.

Validation studies demonstrated that replacing the detailed Jafri et al. (1998) I_{Ca} model with our reduced-order model of I_{Ca} did change the normal time course of the original channel open probability, respectively, I_{Ca} and

$I_{Ca,K}$ (Winslow et al., 1999; Michailova and McCulloch, 2001). To fix this problem we increased the original channel permeability ($\bar{P}_{Ca}$ and P'_k) 1.15-fold. Our calculations (Fig. 2 *B*) show that now the normal time course of subspace Ca^{2+} signal is quite similar in shape, the calculated normal L-type Ca^{2+} current and action potential are only slightly modified, and $[Ca^{2+}]_{ss}$, I_{Ca}, or action-potential time courses in metabolically inhibited conditions are not affected. Because all subsequent simulations yielded very similar results with either approximation, only the simulations using the new reduced-order I_{Ca} model are shown in the Results.

RESULTS

Effects of ATP on $I_{K(ATP)}$ and I_{Ca} currents, contractile activity, and action potential

The first set of the modeling results describes our attempt to create a simulation that quantitatively approximates the reported experimental data for the $[ATP]_i$ dependence of K_{ATP} channel activity in the presence of ADP and Mg^{2+} in guinea pig ventricular myocytes (Nichols et al., 1991a) because we could not find experimental data in canine ventricular myocytes. In these experiments: a), normal $[ATP]_{tot}$, $[ADP]_{tot}$, and $[Mg^{2+}]_i$ were 5 mM, 200 μM, and 0.5 mM; and b), free ATP was omitted from the dialyzing solution, batting the intracellular surface of isolated myocyte, and in this way $[ATP]_{tot}$ was decreased while total intracellular Mg^{2+} and ADP remained unchanged. Fig. 3 *A* shows that the new whole-cell model quantitatively reproduces the experimental data of Nichols et al. (1991a). The calculated relative current ($I_{K(ATP)}/I_{K(ATP=0)}$) in response to rhythmically applied pulses (1-Hz; 9–10 s) approaches one at ~0.01 μM intracellular free ATP (or ~0.5 mM $[ATP]_{tot}$) and is close to zero at ~1 mM $[ATP]_i$ (or ~5.5 mM $[ATP]_{tot}$). Under these conditions, the free model parameters (k_{ATP},k_{MgADP},$G_{K(ATP)}$) were estimated to be 600 μM, 400 μM, and 0.05 mS/μF. The relative conductance g_o (0.08) and g_d (0.89) were taken from Hopkins et al. (1992).

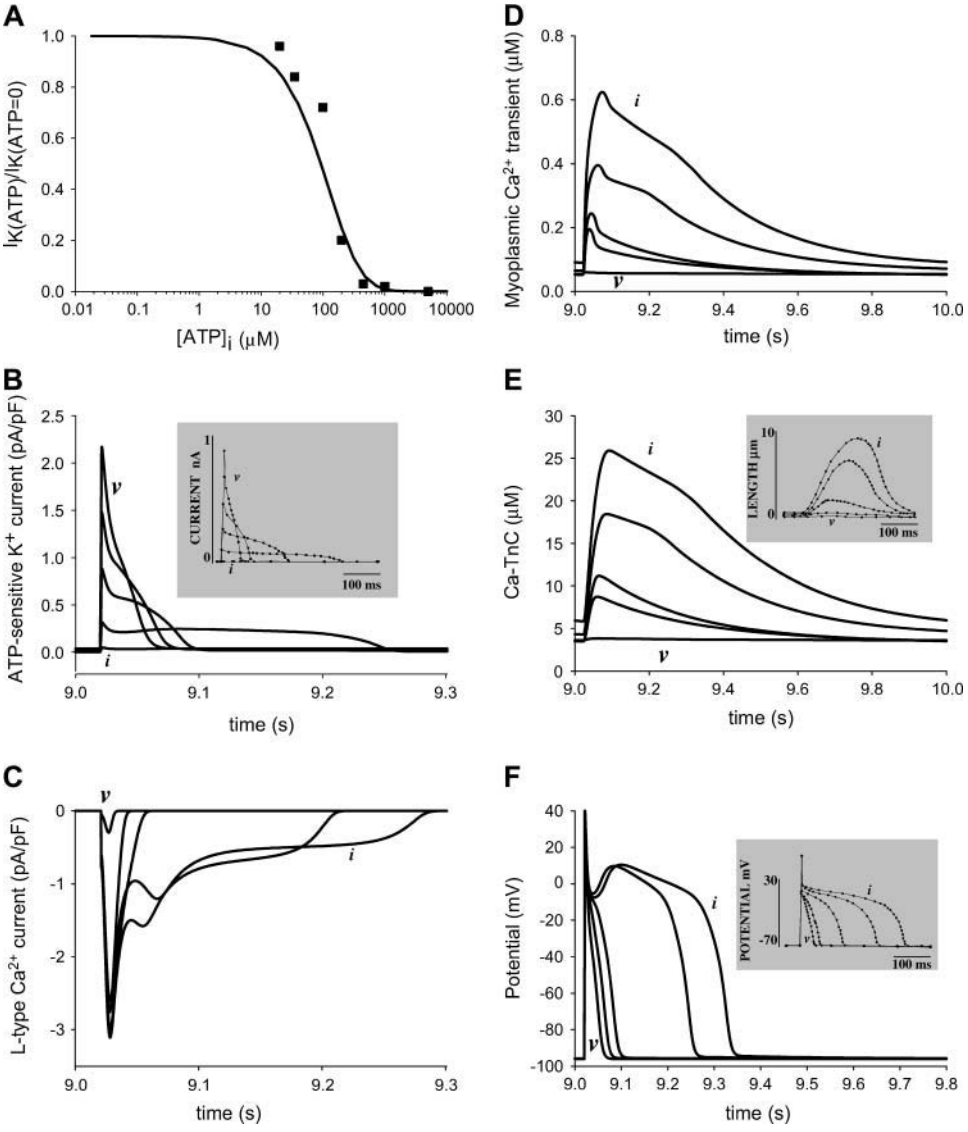

FIGURE 3 Effects of ATP on cardiac EC coupling. (*A*) Dose-response relationship for the effects of free ATP (or total ATP from 0 to 10 mM) on relative K_{ATP} channel current ($I_{K(ATP)}/I_{K(ATP=0)}$). The solid line was fitted to experimental data by Nichols et al. (1991a) (■) with $k_{ATP} = 600$ μM, $k_{MgADP} = 400$ μM, $G_{K(ATP)} = 0.05$ mS/μF, $P_o = 0.08$, $P_d = 0.89$. (*B–F*) Time courses of $I_{K(ATP)}$, I_{Ca}, $[Ca^{2+}]_i$, $[Ca - TnC]_i$, and action potential. Letters (*i–v*) correspond to 5, 4, 3, 2, and 0.5 mM $[ATP]_{tot}$, respectively. Insets show experimental recordings (Fig. 4 *B* in Nichols et al., 1991a) of superimposed $I_{K(ATP)}$ (panel *B*), twitches (panel *E*), and action potentials (panel *F*) for the effects of injection of stimulated K_{ATP} current. Letters (*i–v*) in insets correspond to digitized experimental plots (*i, ii, vii, x, xi*). Simulations are generated in response to 1-Hz pulse and model outputs at the tenth stimulus are shown only. $[ADP]_{tot}$ 200 μM, $[Mg^{2+}]_{tot}$ 4.84 mM, $[K^+]_o$ 4 mM, $[Na^+]_o$ 138 mM, $[Ca^{2+}]_o$ 2 mM.

The effects of metabolic blockade on $I_{K(ATP)}$ and I_{Ca} currents, myoplasmic Ca^{2+} transient, $[Ca-TnC]_i$ time course, and AP shape (9–10 s) are shown in Fig. 3. Simulations with the model suggest that a decrease in total ATP from 5 to 0.5 mM (with $[ADP]_{tot}$ and $[Mg^{2+}]_i$ normal): 1), activated $I_{K(ATP)}$ and shortened current duration (Fig. 3 *B*); 2), declined normal amplitude of $[Ca^{2+}]_i$ and $[Ca-TnC]_i$ peak (Fig. 3, *D–E*); and 3), shortened AP (Fig. 3 *F*). Insets (see Fig. 3, *B* and *E–F*) show that these model predictions resulted in qualitative agreement with experimentally recorded $I_{K(ATP)}$, contractile activity, and AP shape in normoxia and during metabolic inhibition (Fig. 4 *B* in Nichols et al., 1991a). In the published control experiment ($[ATP]_{tot}$ 5 mM, $[ADP]_{tot}$ 200 μM, $[Mg^{2+}]_i$ 0.5 mM), measured action potential duration at −60 mV (APD_{60}) was 302 ± 24 ms (see Fig. 3 *F*, *inset*, plot *i*). The calculated control APD_{60} was ~320 ms (Fig. 3 *F*, plot *i*). Fig. 3 *C* shows that an increase in total ATP from 0.5 to 5 mM (respectively, in $[MgATP]_{ss}$ from 490 μM to 4.26 mM) enhanced I_{Ca} current. The model predictions for the effects of intracellular MgATP on the L-type Ca^{2+} channel activity are in agreement with measurements by O'Rourke et al. (1992) and Yazawa et al. (1997).

Modulation of ATP sensitivity of K_{ATP} channel by ADP in the presence of Mg^{2+}

Experimental studies in rat and guinea pig ventricular myocytes (Lederer and Nichols, 1989; Weiss et al., 1992) suggest that cardiac K_{ATP} channels are regulated by ATP, and that this regulation is sensitive to other intracellular nucleotides, Mg^{2+} and pH. Measuring the ATP dependence of channel activity at different ADP with total ATP and Mg^{2+} constant, Lederer and Nichols (1989) observed that low concentrations of free ADP ($[ADP]_i < 0.5$ mM) increase K_{ATP} channel activity whereas free ADP levels higher than 0.5 mM inhibit channel activity. To test whether the ionic-metabolic model is able to reproduce these experimental data, we calculated $I_{K(ATP)}$ current (5–10 s) in response to 1-Hz periodic pulse by increasing free ADP but keeping total ATP 5 mM (Fig. 4 *A*, *top traces*), 4.9 mM (Fig. 4 *A*, *middle traces*), and 4.5 mM (Fig. 4 *A*, *bottom traces*). During these simulations, free ATP levels ($[ATP]_i$) were 697, 741, and 786 μM (Fig. 4 *A* and Table 1) and total Mg^{2+} was constant at normal level (4.84 mM). Table 1 also shows estimated $[ADP]_{tot}$, $[MgADP]_i$, and $[Mg^{2+}]_i$. The results suggest that: 1), the increase in free ADP, with $[ADP]_i < 0.5$ mM and total ATP 5 or 4.9 mM, activated $I_{K(ATP)}$; 2), the increase in free ADP, with $[ADP]_i > 0.5$ mM and total ATP 4.5 mM, inhibited $I_{K(ATP)}$; and 3), the decrease in total intracellular ATP level (from 5 to 4.5 mM) enhanced $I_{K(ATP)}$ current for all free ADP concentrations.

An advantage of this model is also its ability to simulate and predict how the changes in intracellular ATP in the absence of SUR2A activation ($[ADP]_{tot}$ or $[Mg^{2+}]_{tot}$ 0 mM) regulate $I_{K(ATP)}$ current during a single beat. The simulations (Fig. 4 *B*) revealed that a 1 mM increase or decrease of $[ATP]_{tot}$ from 5 mM (with 0 mM $[ADP]_{tot}$ and 4.84 mM $[Mg^{2+}]_{tot}$) significantly affected the peak of $I_{K(ATP)}$ current and did not influence the current duration. Model results (Fig. 4 *B*) also show that an increase in total ATP from 4 to 6 mM decreased $I_{K(ATP)}$ peak ~30-fold. During this numerical experiment, $[ATP]_i$ increased from ~286 μM to ~1.4 mM and $[Mg^{2+}]_i$ decreased from ~1.13 mM to ~278 μM. In addition, the model predicted that a 1 mM increase or decrease of $[ATP]_{tot}$ from 5 mM, in the presence of 200 μM $[ADP]_{tot}$, but in the absence of Mg^{2+}, totally inhibited $I_{K(ATP)}$ current (not shown). Calculated free ATP levels were 5.99, 4.99, and 3.99 mM, i.e., high enough to block the current via the channel.

The model was also used to simulate how alterations in intracellular ADP or Mg^{2+} in the absence of Kir6.2 inhibition ($[ATP]_{tot} = 0$ mM) regulate $I_{K(ATP)}$ current during a single beat. The simulations indicate that an increase of $[ADP]_{tot}$ from 100 to 300 μM (and of $[MgADP]_i$ from 88 to 262 μM) with intracellular $[Mg^{2+}]_{tot}$ unchanged (~4.84 mM) increased $I_{K(ATP)}$ peak current but these changes did not influence current duration (Fig. 4 *C*). These results also suggested that during current activation, $[Mg^{2+}]_i$ dropped from 4.7 to ~4.6 mM. In addition, the model predicted that a 50% increase or decrease of total Mg^{2+} from 4.84 mM with 200 μM $[ADP]_{tot}$ has a negligible effect on $I_{K(ATP)}$ current (not shown). The calculated $[MgADP]_i$ levels here were 183, 175, and 157 μM.

Effects of total ATP and ADP on cardiac EC coupling

To test the hypothesis that absolute levels of adenine nucleotides ($[ATP]_{tot}$ and $[ADP]_{tot}$) regulate cardiac EC coupling independently of the $[ATP]_{tot}/[ADP]_{tot}$ ratio, we performed another set of calculations, changing total ATP and ADP but keeping $[ATP]_{tot}/[ADP]_{tot}$ (25) and total Mg^{2+} (~4.84 mM) constant. The outputs of the model (10th cycle; 9–10 s) in response to rhythmically applied pulses are shown in Fig. 5. The results showed that a 50% decrease (*dashed-dotted lines*) of $[ATP]_{tot}$ from 5 mM and $[ADP]_{tot}$ from 200 μM were able to affect noticeably the L-type Ca^{2+} current duration, diastolic and systolic $[Ca^{2+}]_i$, $I_{K(ATP)}$ current, and action potential shape whereas a 50% increase (*dashed lines*) enhanced, but not too sensitively, systolic Ca^{2+} peak, prolonged I_{Ca} and action potential, and totally inhibited $I_{K(ATP)}$ current. The predicted $[ATP]_i$, $[MgADP]_i$, $[MgATP]_{ss}$, and $[MgATP]_i$ during this experiment are shown in Table 2. Simulations also showed that the changes in total adenine nucleotide concentrations could markedly influence SR and subspace Ca^{2+} transients and all Ca^{2+}-dependent currents—$I_{NaCa}, I_{Ca,K}, I^*_{p(Ca)}, I_{Ca,b}$ (not shown). Intracellular Na^+ and K^+ concentrations and $I_{Na}, I_{NaK}, I_{Na,b}, I_{Kr}, I_{Ks}, I_{to1}, I_{K1}, I_{Kp}$ were also influenced to some extent, but not greatly (not shown).

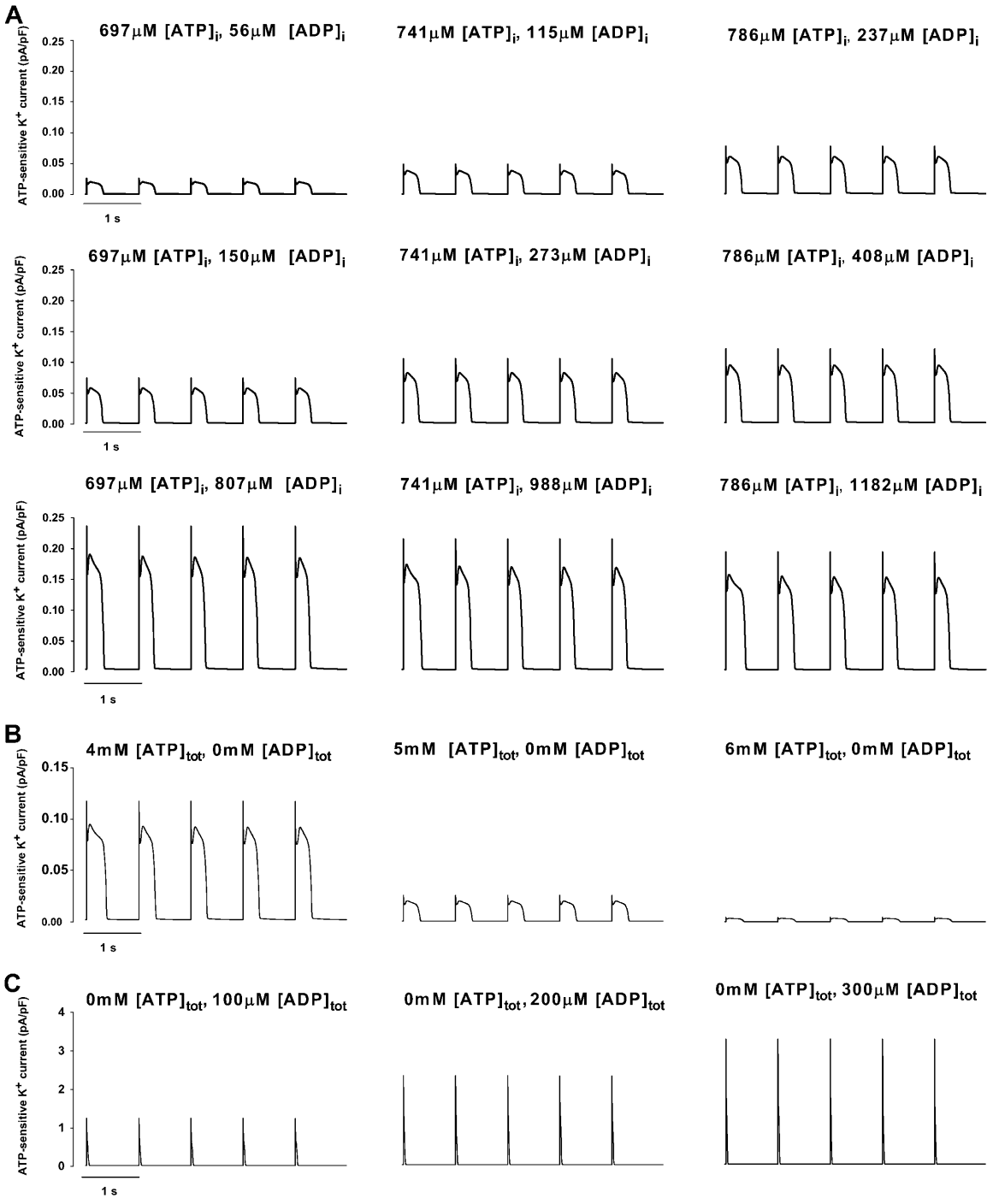

FIGURE 4 Dependence of K_{ATP} channel activity on ADP in the presence of Mg^{2+}. Calculated ATP-sensitive K^+ currents (5–10 s) in response to 1-Hz stimuli are shown. (*A*) Top, middle, and bottom traces show the shift in the sensitivity of K_{ATP} channels to ATP caused by increases in free ADP. (*B*) Effects of 1 mM increase or decrease in total ATP from 5 mM in the absence of ADP on K_{ATP} current. (*C*) Effects of 100 μM increase or decrease in total ADP from 200 μM in the absence of ATP on K_{ATP} current. $[Mg^{2+}]_{tot}$ 4.84 mM, $[K^+]_o$ 4 mM, $[Na^+]_o$ 138 mM, $[Ca^{2+}]_o$ 2 mM.

Effects of cytosolic Mg^{2+} on cardiac EC coupling

Experimental data suggest that magnesium ions play a fundamental role in cellular function, but the effects of alterations in the concentration of intracellular free magnesium ($[Mg^{2+}]_i$) on cardiac EC coupling are poorly understood. The updated ionic-metabolic model provided the opportunity to examine how the variations in intracellular Mg^{2+} ($[Mg^{2+}]_{tot}$, respectively, in $[Mg^{2+}]_i$) may affect $I_{K(ATP)}$, I_{Ca}, and other ionic currents, Ca^{2+} transients, and action potential

TABLE 1 Modulation of ATP sensitivity of K_{ATP} channel by ADP

Total ATP	Free ATP	Total ADP	Cytosolic MgADP	Cytosolic free Mg^{2+}
5 mM (Fig. 4 *A*, *top traces*)	697 μM	10 μM	4.4 μM	537 μM
	741 μM	200 μM	85 μM	500 μM
	786 μM	400 μM	163 μM	467 μM
4.9 mM (Fig. 4 *A*, *middle traces*)	697 μM	267 μM	117 μM	525 μM
	741 μM	470 μM	197 μM	488 μM
	786 μM	682 μM	275 μM	456 μM
4.5 mM (Fig. 4 *A*, *bottom traces*)	697 μM	1374 μM	567 μM	475 μM
	741 μM	1632 μM	644 μM	441 μM
	786 μM	1901 μM	719 μM	411 μM

shape. Simulations with the model revealed that an increase of $[Mg^{2+}]_i$ around the reported physiological concentration range, 0.2–1.8 mM, (Buri and McGuigan, 1990; Hongo et al., 1994; Wang et al., 2003): a), slightly increased the peak of Ca^{2+} current through the L-type channel and markedly shortened current duration (Fig. 6 *A*); b), decreased systolic $[Ca^{2+}]_i$ peak and Ca^{2+} signal at 1.8 mM $[Mg^{2+}]_i$ reached the diastolic level earlier than that at 0.5 mM free Mg^{2+} (Fig. 6 *B*); c), sensitively increased K_{ATP} current peak and decreased current duration (Fig. 6 *C*); and d), significantly shortened action potential duration (Fig. 6 *D*). The model predictions of decreased AP duration in response to enhanced cytosolic Mg^{2+} levels are in qualitative agreement with experimental data (Fig. 6 *D*; *inset* is from Agus et al., 1989). In these studies, total cytosolic ATP and ADP remained constant at normal values ($[ATP]_{tot} = 5$ mM, $[ADP]_{tot} = 200$ μM) and total Mg^{2+} increased from ~3.7 to ~6.7 mM. The predicted $[ATP]_i$, $[MgADP]_i$, $[MgATP]_{ss}$, and $[MgATP]_i$ here are shown in Table 3. In addition, the variations in intracellular Mg^{2+} sensitively affected the diastolic and systolic SR Ca^{2+} levels, $[Ca^{2+}]_{ss}$ signal, the efficiency of Na^+/Ca^{2+} exchanger, $I_{Ca,K}$, $I^*_{p(Ca)}$, and $I_{Ca,b}$ currents whereas $[Na]_i$, $[K]_i$, I_{Na}, I_{NaK}, $I_{Na,b}$, I_{Kr}, I_{Ks}, I_{to1}, I_{K1}, and I_{Kp} remained essentially unchanged (not shown).

Metabolic inhibition

In cardiomyocytes, Weiss et al. (1992) reported that during ischemia: 1), average cytosolic ATP remains in the millimolar range (normoxia ~ 6.8 mM; 40-s ischemia ~ 5.4 mM; 10-min ischemia ~ 4.6 mM); 2), free cytosolic ADP increases from 15 to 30 or 99 μM after 40-s or 10-min ischemia; and 3), total Mg^{2+} dose not change whereas normal $[Mg^{2+}]_i$ increases (normal free Mg^{2+} ~ 2mM). To examine how the reported changes in $[ATP]_{tot}$ and $[ADP]_i$ during ischemia might affect

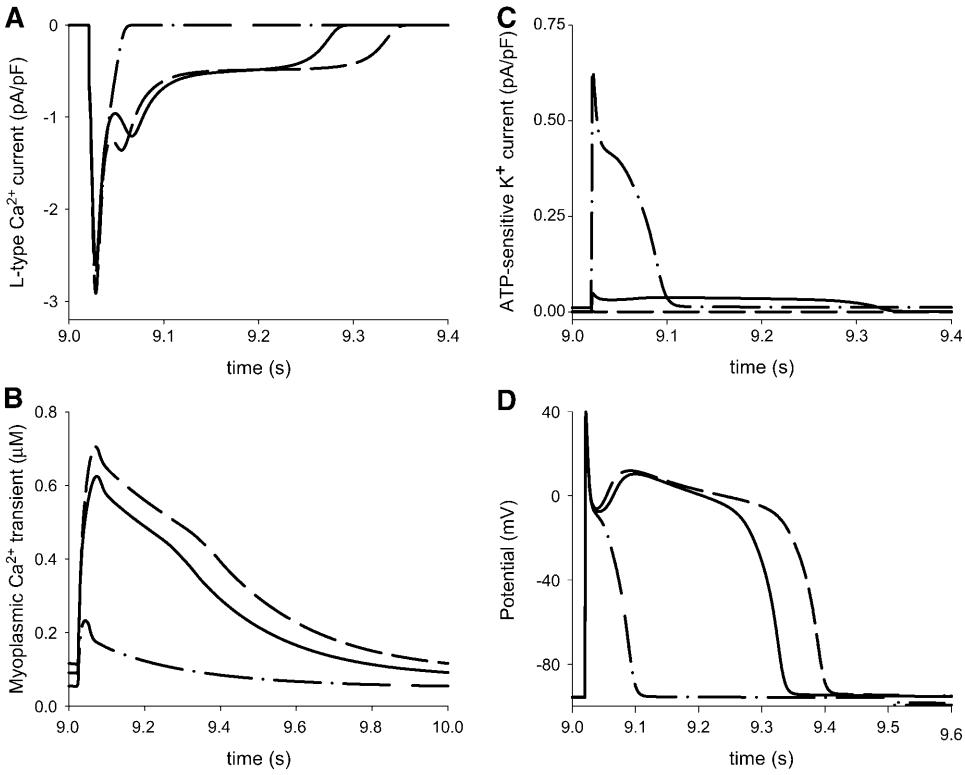

FIGURE 5 Absolute levels of ATP and ADP regulate cardiac EC coupling independently of ATP/ADP ratio. Panels *A–D* show effects of 50% simultaneous increase or decrease in total ATP and total ADP with $[ATP]_{tot}/[ADP]_{tot}$ unchanged on I_{Ca}, $[Ca^{2+}]_i$, $I_{K(ATP)}$, and action potential (9–10 s) in response to 1-Hz periodic pulse. (*Dashed line*) $[ATP]_{tot}$ 7.5 mM, $[ADP]_{tot}$ 300 μM. (*Solid line*) $[ATP]_{tot}$ 5 mM, $[ADP]_{tot}$ 200 μM. (*Dashed-dotted line*) $[ATP]_{tot}$ 2.5 mM, $[ADP]_{tot}$ 100 μM. Total Mg^{2+} ~ 4.84 mM, ATP/ADP = 25.

TABLE 2 Effects of total ATP and ADP

Total ATP and ADP	Free ATP	Cytosolic Mg ADP	Subspace MgATP	Cytosolic MgATP
7.5 mM $[ATP]_{tot}$ 300 μM $[ADP]_{tot}$	2.85 mM	52 μM	4.65 mM	4.65 mM
5 mM $[ATP]_{tot}$ 200 μM $[ADP]_{tot}$	741 μM	85 μM	4.26 mM	4.26 mM
2.5 mM $[ATP]_{tot}$ 100 μM $[ADP]_{tot}$	89 μM	78 μM	2.4 mM	2.4 mM

$I_{K(ATP)}$ and I_{Ca} current as well cardiac EC coupling we performed another set of calculations (Fig. 7). Model results showed that a fall in $[ATP]_{tot}/[ADP]_{tot}$ ratio (from 114 to 31 or 7) with total Mg^{2+} constant significantly decreased action potential duration (Fig. 7 *H*). In addition, our studies showed that block of oxidative metabolism increased $I_{K(ATP)}$ and I_{Ca} current peaks and shortened current durations, reduced sarcoplasmic Ca^{2+} content, lowered systolic Ca^{2+} and Ca-TnC peaks, and decreased the efficiency of the Na^+/Ca^{2+} exchanger in extruding Ca^{2+} (Fig. 7, *A–G*). Predicted $[ATP]_i$, $[MgATP]_i$, $[MgATP]_{ss}$, $[ADP]_{tot}$, $[MgADP]_i$, and $[Mg^+]_i$ in normal conditions and after 40-s and 10-min ischemia are shown in Table 4. In contrast to the significant changes in $I_{Ca,K}$, $I^*_{p(Ca)}$, and $I_{Ca,b}$ the predicted effects of metabolic inhibition on I_{NaK}, I_{Na}, I_{K1}, and $I_{Na,b}$ currents were negligible (not shown). The normal time courses of I_{Kr}, I_{Ks}, I_{to1}, and I_{Kp} remained almost unchanged after 10-s stimulation (not shown).

DISCUSSION

K_{ATP} channel model

Taking into consideration experimental data (Ashcroft and Gribble, 1998; Gribble et al., 2000; Ribalet et al., 2003)—Kir6.2 subunit is the primary site at which intracellular free ATP acts to cause K_{ATP} channel inhibition while SUR2A subunit mediates the stimulatory effects of intracellular MgADP and there are no gradients observed between bulk cytosolic and submembrane ATP—we postulated in the model that the changes in myoplasmic ATP and MgADP regulate K_{ATP} current. Experimental studies also indicate that Kir6.2 and SUR2A subunits coassemble in an obligate 4:4 stoichiometry to form the octameric channel and that the binding of only one molecule ATP is sufficient to close the channel whereas it is not known whether the interaction of one or two MgADP molecules with only one of the four SUR2A subunits is sufficient to increase the channel activation (Nichols et al., 1996c; Gribble et al., 1997; Ueda et al., 1997; Ashcroft and Gribble, 1998). Therefore, in this study we tested the hypotheses that: 1), there are four sites that bind ATP but only a single ATP molecule needs to bind to cause channel closure, and 2), the simultaneous binding of two MgADP molecules to one of SUR2A subunit is required to increase channel open probability. Finally, we also assumed that there are two populations of sarcolemmal K_{ATP} channels open.

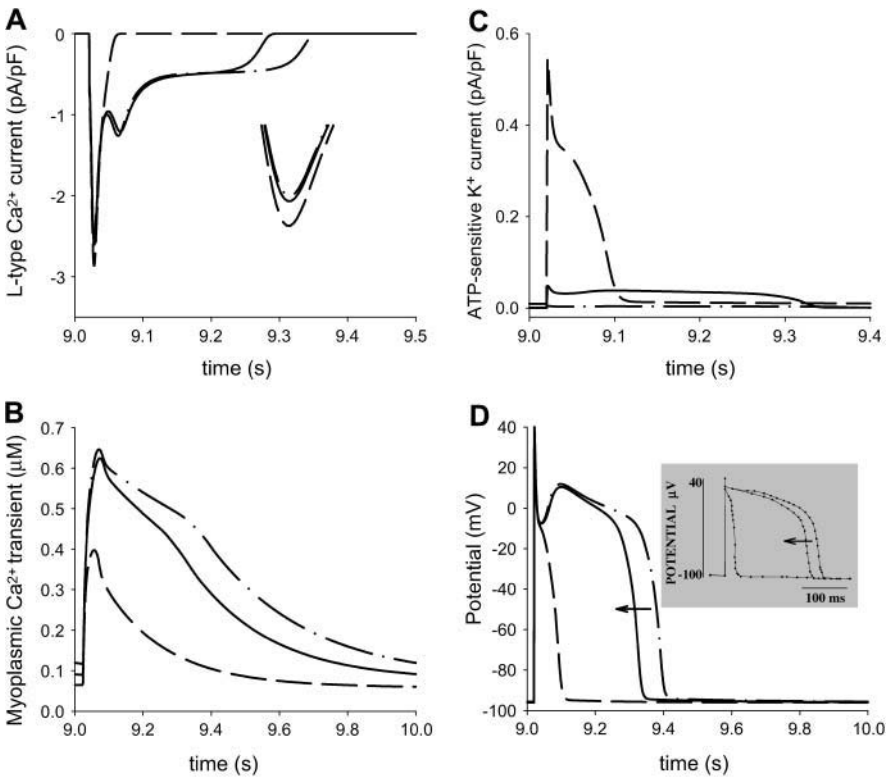

FIGURE 6 Effects of cytosolic Mg^{2+} on cardiac EC coupling. Panels *A–D* show effects of changes in cytosolic Mg^{2+} on I_{Ca}, $[Ca^{2+}]_i$, $I_{K(ATP)}$, and action potential (9–10 s) in response to 1-Hz periodic pulse. (*Dashed-dotted line*) $[Mg^{2+}]_i$ 0.2 mM, total Mg^{2+} 3.73 mM. (*Solid line*) $[Mg^{2+}]_i$ 0.5 mM, total Mg^{2+} 4.84 mM. (*Dashed line*) $[Mg^{2+}]_i$ 1.8 mM, total Mg^{2+} 6.7 mM. Total ATP 5 mM, total ADP 200 μM. Bottom trace in panel *A* shows an expanded view of the peak of L-type Ca^{2+} current. Inset in panel *D* is from Agus et al. (1989) and shows the suppressive effect of elevated Mg^{2+} levels on the experimentally recorded action potentials. The first, second, and last experimental plots (*right to left*) are digitized.

TABLE 3 Effects of cytosolic Mg^{2+}

Cytosolic free Mg^{2+}	Free ATP	Cytosolic MgADP	Subspace MgATP	Cytosolic MgATP
0.2 mM	1.5 mM	46 μM	3.5 mM	3.5 mM
0.5 mM	741 μM	85 μM	4.26 mM	4.26 mM
1.8 mM	230 μM	145 μM	4.8 mM	4.8 mM

We need to acknowledge here that ours is not the only model of ATP and MgADP regulation of the K_{ATP} channel availability. Hopkins et al. (1992) proposed a model of channel-nucleotide interaction with two kinds of ADP binding sites, regulating sarcolemmal K_{ATP} channel in mouse pancreatic β-cells. In that model, one site specifically binds two MgADP molecules and increases channel opening. The other site binds either one molecule ATP or ADP and decreases channel opening. Recently, Ashcroft and Gribble (1998) showed also that the four-site ATP model was able to fit better their ATP dose-response experimental data than the one-site ATP model. Therefore, there were several reasons why the new formulation for the dependence of aggregate channel availability on nucleotide concentrations ($f_{K(ATP)}$) was necessary: 1), the K_{ATP} channel is the octameric structure containing four Kir6.2 and four SUR2A subunits, not assumed in the Hopkins et al. (1992) model; 2), Kir6.2 subunit is the primary site for ATP binding only and not for ADP; and 3), MgADP probably interacts with both SUR2A NBDs, so that two molecules MgADP bind to each SUR2A subunit.

Furthermore, we need to stress that the gating kinetics of the single K_{ATP} channel is not included into our ionic-metabolic model yet. Experimental and theoretical studies (Spruce et al., 1987; Gillis et al., 1989; Davies, 1990; Davies et al., 1991, 1992; Nichols et al., 1991b; Alekseev et al., 1997; Trapp et al., 1997; Karschin et al., 1998) suggest that the kinetic behavior of K_{ATP} channel is complex, i.e., that the first ATP molecule is assumed to close the channel but subsequent ATP binding might then stabilize blocked channel or that MgADP binding to SUR2A subunit may affect the binding or action of ATP on Kir6.2 ATP site. A kinetic model of the ATP-dependent regulation of channel activity, based on the assumption of four sequential ATP-binding states, was suggested by Nichols et al. (1991b) for rat ventricular myocytes. The model assumes one ATP-independent open state, one ATP-dependent open state, one ATP-independent closed state as well as four ATP-dependent closed states reflecting the sequential binding of four ATP molecules to the channel. The binding of the first ATP molecule is assumed to close the channel and subsequent ATP binding might then stabilize the blocked channel.

Ca^{2+} channel model

To formulate the reduced-order Ca^{2+} channel gating model, we used the detailed Markov model (Jafri et al., 1998). We found that the channel subunit interactions influence sensitively channel open probability. For this reason we fit the Winslow et al. (1999) whole-cell Ca^{2+} current by increasing channel permeability for Ca^{2+} and K^+ ions 1.15-fold. We concluded that the observed differences during I_{Ca} current inactivation in normal conditions were probably due to limitations of assumptions: i), voltage-independent activation gating occurs independently of the voltage-dependent conformational changes in the subunits; ii), transitions between normal and Ca^{2+}-inactivated modes occur much more slowly than voltage-dependent gating within a mode. Furthermore, in agreement with experimental data (O'Rourke et al., 1992; Yazawa et al., 1997)—MgATP regulates directly cardiac Ca^{2+} channel through a phosphorylation-independent mechanism—we assumed the channel availability (f_{Ca}) depending on subspace MgATP concentration. Our studies revealed that both approaches yield similar results under a variety of pathological conditions.

Cardiac K_{ATP} and L-type Ca^{2+} currents, cytosolic Mg^{2+}, adenine nucleotide phosphates, and EC coupling

The whole-cell model was able to simulate quantitatively or qualitatively various experimental measurements in normal and pathological conditions and to make predictions that are possible to test experimentally. The most important theoretical result was our observation that the changes in normal diastolic free ATP, MgADP, and MgATP concentrations, as a consequence of the changes in absolute cytosolic Mg^{2+}, ATP, and ADP levels regulate the K_{ATP} and L-type Ca^{2+} channel activity and the integrated process of excitation-contraction coupling in ventricular myocytes. In addition, model studies demonstrated (see also Michailova and McCulloch, 2001) that the changes in intracellular Ca^{2+} concentrations ($[Ca^{2+}]_i$ and $[Ca^{2+}]_{ss}$) during cell excitation were not able to cause sensitive alterations in the diastolic free ATP, MgADP, and MgATP normal or pathological level.

Calculations showed that the current model quantitatively reproduces Nichols et al. (1991a) metabolic experiments on $[ATP]_i$ dependence of K_{ATP} channel activity in the presence of normal $[ADP]_{tot}$ and $[Mg^{2+}]_{tot}$. However, the model was able only qualitatively to simulate the effects of metabolic blockade on $I_{K(ATP)}$ and AP time courses during a single beat. The analysis suggests that the enhanced K_{ATP} current and markedly shortened current and AP-potential durations, were due to decreased free diastolic ATP and increased diastolic MgADP level. In addition, results revealed that the drop in total ATP inhibited Ca^{2+} signal and consequently contractile activity (in this article we assume contractile force $f \sim [Ca - TnC]_i$). The analysis suggests that the most important reason for this was the downregulation of SERCA2a pump by the reduced diastolic MgATP levels. Here, we hypothesize that the experimentally recorded

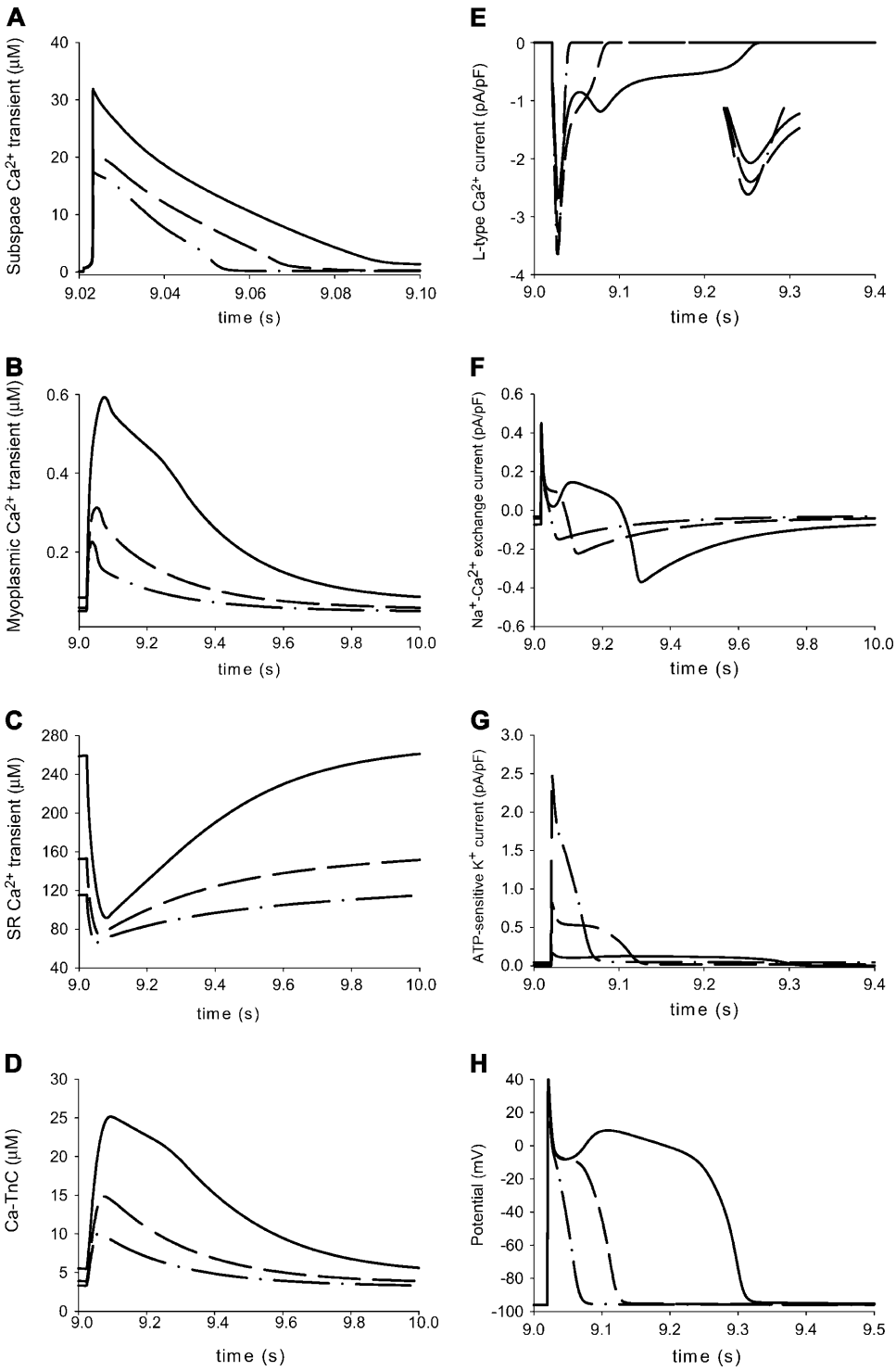

FIGURE 7 Panels *A–H* show model outputs in response to 1-Hz periodic pulse (9–10 s). Bottom trace in panel *E* shows an expanded view of the peak of L-type Ca^{2+} current. Normal conditions are $[ATP]_{tot}$ 6.8 mM, $[ADP]_i$ 15 μM, $[Mg^{2+}]_i$ 2 mM (*solid line*). Ischemia (40 s) is $[ATP]_{tot}$ 5.4 mM, $[ADP]_i$ 30 μM, $[Mg^{2+}]_i$ 3.165 mM (*dashed line*). Ischemia (10 min) is $[ATP]_{tot}$ 4.6 mM, $[ADP]_i$ 99 μM, $[Mg^{2+}]_i$ 3.55 mM (*dashed-dotted line*). Total Mg^{2+} 8.56 mM.

twitches (Nichols et al., 1991a) reach maximum amplitude slower than calculated because actin and myosin interactions as well MgATP regulation of myosin ATP-ase are not included in the model, yet. Finally, this model was able to simulate qualitatively the effects of rapid increase in intracellular diastolic MgATP on Ca^{2+} channel activity (O'Rourke et al., 1992; Yazawa et al., 1997).

An interesting feature of this model was its ability to simulate the modulation of ATP sensitivity of K_{ATP} channel by ADP in the presence of Mg^{2+}. Our studies demonstrated that at all $[ADP]_i$ concentrations below 500 μM (with total Mg^{2+} normal), the increase in ADP stimulated channel activity. However, at all $[ADP]_i$ concentrations >500 μM, the increase in ADP caused channel inhibition. How could

TABLE 4 Metabolic inhibition

	Normoxia	Ischemia (40 s)	Ischemia (10 min)
Free ATP	283.5 μM	144.5 μM	110 μM
Cytosolic MgATP	6.51 mM	5.25 mM	4.49 mM
Subspace MgATP	6.51 mM	5.25 mM	4.49 mM
Total ADP	59.5 μM	170.5 μM	619.5 μM
Cytosolic MgADP	44.5 μM	140.5 μM	520.4 μM
Cytosolic free Mg^{2+}	2 mM	3.165 mM	3.55 mM

we explain these ''paradoxical ADP effects'' on the channel activity? The simulations here revealed that for $[ADP]_i < 500$ μM the $[ATP]_i/[ADP]_i$ ratio was greater than unity and $[MgADP]_i \ll [ATP]_i$. In contrast, for all $[ADP]_i > 500$ μM the $[ATP]_i/[ADP]_i$ ratio was below unity and $[MgADP]_i \approx [ATP]_i$. In addition, calculations showed that in both cases the diastolic MgADP increased and $[ATP]_{tot}/[ADP]_{tot} > 1$. Therefore, we concluded that in cardiac myocytes, a high level of free ADP would be expected to cause channel inhibition when $[ATP]_i/[ADP]_i < 1$ (or $[ATP]_i < [ADP]_i$). Our predictions for the effects of ADP in modulating ATP sensitivity of K_{ATP} channel are in agreement with reported experimental data in rat and guinea pig myocytes (Lederer and Nichols, 1989; Weiss et al., 1992). To explain the observed ''paradoxical ADP effect'' Lederer and Nichols (1989) hypothesize that total ADP becomes greater than total Mg^{2+} with $[ADP]_i > 500$ μM. Our studies showed that here $[ADP]_{tot} < [Mg^{2+}]_{tot}$.

This model is also able to predict how the changes in cytosolic ATP in the absence of SUR2A activation (ADP or Mg^{2+} 0 mM) or the changes in cytosolic ADP or Mg^{2+} in the absence of Kir6.2 inhibition (ATP 0 mM) regulate $I_{K(ATP)}$ current. Computations showed that, in the absence of ADP and presence of Mg^{2+}, the increase of total ATP (or $[ATP]_i$) significantly inhibited $I_{K(ATP)}$ current. In contrast, in the absence of ATP and presence of Mg^{2+}, the increase of total ADP (or $[MgADP]_i$) sensitively activated $I_{K(ATP)}$ current through the channel. These model predictions are in qualitative agreement with experimental data by Lorenz et al. (1998) in pancreatic K_{ATP} channels. However, we could not find experimental measurements in the literature for $[ATP]_i$ or $[MgADP]_i$ regulation alone of cardiac $I_{K(ATP)}$ current.

It is commonly expressed that excitability and contractility are determined by $[ATP]_{tot}/[ADP]_{tot}$ ratio. By testing this, we demonstrated that the absolute levels of adenine nucleotides regulate K_{ATP} and L-type Ca^{2+} channel activity and cardiac EC coupling independently of the $[ATP]_{tot}/[ADP]_{tot}$ ratio. Our model predicts that simultaneous decrease in $[ATP]_{tot}$ and $[ADP]_{tot}$ (with total Mg^{2+} unchanged) activate K_{ATP} current, do not affect I_{Ca} peak, inhibit $[Ca^{2+}]_i$ signal, and markedly shorten action potential, $I_{K(ATP)}$ and I_{Ca} current durations. The analysis suggests that observed changes in myoplasmic Ca^{2+} signal and I_{Ca} were due to the changes in diastolic $[MgATP]_i$ and $[MgATP]_{ss}$ whereas those in $I_{K(ATP)}$ current due to the alterations in diastolic $[ATP]_i$ and $[MgADP]_i$. Therefore, our data and those of others (Dunne et al., 1988; Albitz et al., 1990) reveal that understanding of the control of K_{ATP} and L-type Ca^{2+} channel activities and of the integrated EC coupling process requires knowing more metabolic variables than the $[ATP]_{tot}/[ADP]_{tot}$ ratio. New electrophysiological measurements in cardiac myocytes need to be done to test further the $[ATP]_{tot}/[ADP]_{tot}$ ratio hypothesis and the correctness of our model predictions.

Despite of the fact that Mg^{2+} is the most abundant divalent cation in the cell, little is known about intracellular Mg^{2+} homeostasis and mechanisms controlling $[Mg^{2+}]_i$ (Murphy, 2000). The absence of detectable major changes in $[Mg^{2+}]_i$ and the slower turnover of the cation across the cell membrane in normal conditions have supported for more than three decades the assumption that total Mg^{2+} content is kept constant at the level necessary for enzyme and channel function, and that its concentration need not change rapidly to form complexes with ATP and other phosphonucleotides. However, a body of new experimental results now suggests that large fluxes of Mg^{2+} can cross the cell membrane in either direction (via electroneutral Na^+/Mg^{2+} exchanger or selective Mg^{2+} channels) following a variety of hormonal and nonhormonal stimuli and inducing sensitive changes in total Mg^{2+} and little or no change in free cytosolic Mg^{2+} (Romani and Scarpa, 1990, 2002; Fatholahi et al., 2000). Here our new model provided a unique opportunity for the first time to investigate theoretically how simultaneous variations in intracellular Mg^{2+} ($[Mg^{2+}]_{tot}$ or $[Mg^{2+}]_i$) may affect Ca^{2+} transients, sarcolemmal K_{ATP} current, and other ionic currents involved in action potential genesis. Computations showed that the changes in $[Mg^{2+}]_i$ (respectively in total Mg^{2+}), even around the reported range of physiological concentrations (0.2–1.8 mM) with total ATP and ADP normal, may have pronounced effect on $I_{K(ATP)}$, on Ca^{2+} signals and the time course of the action potential. The analysis suggests that the main reason for the observed effects were the alterations in normal free ATP, MgADP, and MgATP levels. Our prediction that the increase in $[Mg^{2+}]_i$ leads to shortening of action potential duration is in a qualitative agreement with experimental data by Agus et al. (1989). In addition, experimental data suggest that free Mg^{2+} and Mg^{2+}-nucleotide complexes may exert opposite effects on L-type Ca^{2+} current, i.e., increases in MgATP activate I_{Ca} whereas increases in $[Mg^{2+}]_i$ inhibit the current (O'Rourke et al., 1992). Our calculations showed that the increase in $[MgATP]_{ss}$ increased I_{Ca} peak. However, the model failed to predict that an increase in $[Mg^{2+}]_i$ dramatically suppresses the L-type Ca^{2+} current (Agus et al., 1989; Pelzer et al., 2001; Yamaoka et al., 2002; Wang et al., 2003). Recent experimental studies by Wang et al. (2003) in rat cardiac myocytes suggest that the interaction between $[Ca^{2+}]_i$ and $[Mg^{2+}]_i$ to modulate I_{Ca} is not significantly affected by ryanodine, fast Ca^{2+} buffers, or inhibitors of calmodulin, calmodulin-dependent kinase, and

calcineurin. The authors concluded that physiologically relevant $[Mg^{2+}]_i$ modulates I_{Ca} by counteracting the effects of Ca^{2+} channel phosphorylation or by an unknown $[Ca^{2+}]_i$-dependent mechanism.

Block of oxidative metabolism and a fall in $[ATP]_{tot}/[ADP]_{tot}$ cause significant changes in ion concentrations ($[K^+]_0$, $[H^+]_i$, $[Na^+]_i$, $[Ca^{2+}]_i$, $[Mg^{2+}]_i$) and have important effects on ion channels and carriers (Lederer and Nichols, 1989; Isenberg et al., 1993; Ch'en et al., 1998; Carmeliet, 1999; Bers, 2001). Weiss et al. (1992) report that, while creatine phosphate is present intracellular ATP and ADP remain unchanged but once ATP is depleted a large positive increase in free myoplasmic ADP is observed because the later arises from the hydrolysis of ATP. In this article we examined how the changes in total ATP and free ADP reported by Weiss et al. after 40s of 10 min ischemia might affect the normal cell excitability and contractility. Simulations with the model demonstrated that a fall in $[ATP]_{tot}/[ADP]_{tot}$ (with total Mg^{2+} normal) significantly reduces sarcoplasmic Ca^{2+} content, increases diastolic Ca^{2+}, lowers systolic Ca^{2+}, increases Ca^{2+} influx through L-type channels, and decreases the efficiency of the Na^+/Ca^{2+} exchanger in extruding Ca^{2+} (Isenberg et al., 1993; Carmeliet, 1999). These simulations also resulted in a sensitive decrease of action potential duration, significant activation of ATP-sensitive K^+ current, and an increase of free Mg^{2+} that has been experimentally observed during ischemia (Carmeliet, 1999). Our analysis suggests that the most important reasons for the observed changes during metabolic inhibition were: 1), the downregulation of SERCA2a pump activity by the reduced diastolic MgATP, and 2), the activation of $I_{K(ATP)}$ current due to decreased free ATP and increased MgADP levels.

CONCLUSIONS

Cytosolic free Mg^{2+} and cytosolic ATP, MgATP, ADP, and MgADP regulate a large number of cellular processes. The improved ionic-metabolic model allowed us to investigate how the changes in free and bound Mg^{2+}, ATP, and ADP during cell excitation regulate the availability of ATP-sensitive K^+ and L-type Ca^{2+} channels and the integrated process of excitation-contraction coupling in ventricular myocytes. The model was able to reproduce quantitatively or qualitatively a sequence of events that corresponds well with experimental data in normal and pathological conditions. However, we need to acknowledge here that this comprehensive whole-cell model has limitations: 1), the assumptions made about the kinetic mechanisms of action of nucleotides at the subunits of the K_{ATP} channel have to be further tested against much more extensive experimental data; 2), the Jafri et al. (1998) L-type Ca^{2+} current model was inspired by certain features of the data of Imredy and Yue (1994), but neither this nor any other gating scheme for L-type channel has been quantitatively validated by single channel measurements; 3), the present L-type Ca^{2+}current model does not account for the effects of Mg^{2+} on this channel; 4), the Winslow et al. (1999) model dose not take into account the realistic gating properties of the RyR that are also strongly modulated by adenine nucleotides and Mg^{2+}; and 5), our current model includes mechanisms of Mg^{2+} handling but these mechanisms are not very well understood at the whole-cell level yet. Therefore, we will further test the model in much greater detail and will extend it to investigate the mechanisms underlying the gating kinetics of K_{ATP} channel, Mg^{2+} regulation of L-type Ca^{2+} channel as well as Mg^{2+}, ATP, and ADP regulation of RyRs, myosin ATPase, SERCA2a pump, Na^+-K^+ ATPase, Na^+/Ca^{2+} exchange, and various other pump and currents involved in action potential genesis (O'Rourke et al., 1992; Hilgemann et al., 1992; Valdivia et al., 1995; Xu et al., 1996; Laver et al., 1997; Berberian et al., 1998; DiPolo and Beauge, 1999; Wei et al., 2002; Wang et al., 2003; Zahradnikova et al., 2003; Tamargo et al., 2004; Ravens et al., 2004; Eisner et al., 2004).

APPENDIX I: MICHAILOVA-McCULLOCH IONICMETABOLIC MODEL

Equations describing Ca^{2+} and Mg^{2+} buffering and transport by ATP and ADP in the subspace and myoplasm:

$$[B_m]_{pool} = [B_m]_{tot} - [CaB_m]_{pool} - [MgB_m]_{pool}$$

$$\frac{d[CaB_m]_{pool}}{dt} = \pm J_{xfer}^{CaB_m} V_{pool} + k_+^{CaB_m}[Ca^{2+}]_{pool}[B_m]_{pool} - k_-^{CaB_m}[CaB_m]_{pool}$$

$$\frac{d[MgB_m]_{pool}}{dt} = \pm J_{xfer}^{MgB_m} V_{pool} + k_+^{MgB_m}[Mg^{2+}]_{pool}[B_m]_{pool} - k_-^{MgB_m}[MgB_m]_{pool}$$

$$\frac{d[Mg^{2+}]_{pool}}{dt} = \pm J_{xfer}^{Mg} V_{pool} - \sum_m \left(k_+^{MgB_m}[Mg^{2+}]_{pool}[B_m]_{pool} - k_-^{MgB_m}[MgB_m]_{pool} \right).$$

B_m represents ATP or ADP; *pool* represents subspace or myoplasm; $k_\pm^{CaB_m}$ and $k_\pm^{MgB_m}$ are on- and off-rate constants for Ca^{2+} and Mg^{2+} binding to ATP or ADP; $\pm J_{xfer}^{CaB_m}$, $\pm J_{xfer}^{MgB_m}$, and $\pm J_{xfer}^{Mg}$ are fluxes for Ca^{2+} and Mg^{2+} bound to ATP or ADP and free Mg^{2+} from subspace to myoplasm; V_{pool} is the scaling factor accounting for the different volumes of subspace and myoplasm.

Modified Winslow et al. (1999) equations for sarcolemmal Ca^{2+} pump current, SERCA2a pump flux, and free subspace and myoplasmic Ca^{2+} concentrations:

$$I_{p(Ca)}^*(t) = \frac{[MgATP]_i}{[MgATP]_{i0}} I_{p(Ca)}(t)$$

$$J_{up}^*(t) = \frac{[MgATP]_i}{[MgATP]_{i0}} J_{up}(t)$$

$$\frac{d[Ca^{2+}]_{ss}}{dt} = \beta_{ss}\left\{J_{rel}\frac{V_{JSR}}{V_{ss}} - J_{xfer}\frac{V_{myo}}{V_{ss}} - (I_{Ca})\frac{A_{cap}C_{sc}}{2V_{ss}F} - \sum_{m}\left(k_{+}^{CaB_m}[Ca^{2+}]_{ss}[B_m]_{ss} - k_{-}^{CaB_m}[CaB_m]_{ss}\right)\right\}$$

$$\frac{d[Ca^{2+}]_{i}}{dt} = \beta_{i}\left\{J_{xfer} - J_{up}^{*} - J_{trpn} - \left(I_{Ca,b} - 2I_{NaCa} + I_{p(Ca)}^{*}\right)\frac{A_{cap}C_{sc}}{2V_{myo}F} - \sum_{m}\left(k_{+}^{CaB_m}[Ca^{2+}]_{i}[B_m]_{i} + k_{-}^{CaB_m}[CaB_m]_{i}\right)\right\}$$

$[MgATP]_{i0}$is diastolic myoplasmic MgATP concentration in normal conditions; β_{ss} and β_i are rapid buffering approximation factors for calmodulin in subspace and myoplasm; A_{cap} is capacitive membrane area; C_{sc} is specific membrane capacity; F is Faraday's constant; J_W, V_W, I_W are fluxes, volumes, and currents as described by Winslow et al. (1999).

APPENDIX II: GLOSSARY

Membrane currents are: I_{Na}, Na^+ current; I_{Kr}, rapid-activating delayed rectifier K^+ current; I_{Ks}, slow-activating delayed rectifier K^+ current; I_{to1}, transient outward K^+ current; I_{K1}, time-independent K^+ current; I_{Kp}, plateau K^+ current; I_{NaCa}, Na^+-Ca^{2+} exchanger current; I_{NaK}, modified Na^+-K^+ pump current; $I_{p(Ca)}^{*}$, modified sarcolemmal Ca^{2+} pump current; $I_{Ca,b}$, Ca^{2+} background current; $I_{Na,b}$, Na^+ background current.

Concentrations are: $[K^+]_o$, extracellular K^+ concentration; $[Ca^{2+}]_o$, extracellular Ca^{2+} concentration; $[Na^+]_i$, intracellular Na^+ concentration; $[K^+]_i$, intracellular K^+ concentration; $[Ca^{2+}]_{ss}$, free subspace Ca^{2+} concentration; $[Ca^{2+}]_i$, free myoplasmic Ca^{2+} concentration; $[Mg^{2+}]_{tot}$, total Mg^{2+} concentration; $[Mg^{2+}]_i$, free myoplasmic Mg^{2+} concentration; $[ATP]_{tot}$, total ATP concentration; $[ATP]_i$, free myoplasmic ATP concentration; $[MgATP]_{ss}$, subspace concentration of Mg^{2+}-bound ATP; $[MgATP]_i$, myoplasmic concentration of Mg^{2+}-bound ATP; $[ADP]_{tot}$, total ADP concentration; $[ADP]_i$, free myoplasmic ADP concentration; $[MgADP]_i$, myoplasmic concentration of Mg^{2+}-bound ADP; $[Ca-TnC]_i$, myoplasmic concentration of Ca^{2+} bound to TnC.

K_{ATP} channel abbreviations and parameters are: K_{ATP}, ATP-sensitive K^+ channel; Kir6.2, inwardly rectifying K^+ channel subunit; SUR2A, regulatory sulphonylurea receptor subunit; NBD, SUR2A nucleotide binding domain; $I_{K(ATP)}$, ATP-sensitive K^+ current; $g_{K(ATP)}$, whole-cell K_{ATP} conductance; $G_{K(ATP)}$, maximum K_{ATP} channel conductance at 0 mM $[ATP]_i$; $f_{K(ATP)}$, aggregate fraction of K_{ATP} channels open; f_{ATP}, fraction of K_{ATP} channels open because there is no ATP molecule bound; f_{MgADP}, fraction of K_{ATP} channels open because there are 2MgADP molecules bound; k_{ATP}, constant at which half of the ATP sites will be occupied; k_{MgADP}, constant at which half of the MgADP sites will be occupied; g_o, relative conductance; g_d, relative conductance; V, membrane potential; E_K, K^+ reversal potential.

I_{Ca} channel abbreviations and parameters are: I_{Ca}, L-type Ca^{2+} channel current; $I_{Ca,K}$, K^+ current through L-type Ca^{2+} channel; v, voltage-dependent activation gate, mode Normal; w, voltage-dependent activation gate, mode Ca; x, voltage-independent activation gate; y, voltage-dependent inactivation gate; z, Ca^{2+}-dependent inactivation gate; P_{rom}, L-type channel open probability; f_{Ca}, relative fraction of available L-type Ca^{2+} channels; $k_{MgATPss}$, constant at which half of MgATP binding sites are occupied; $\bar{P}_{Ca}$, L-type Ca^{2+} channel permeability to Ca^{2+}, P'_K, L-type Ca^{2+} channel permeability to K^+, C_{sc}, specific membrane capacity; F, Faraday constant; R, ideal gas constant; T, absolute temperature.

We thank the reviewers of the manuscript for useful suggestions.

This work was supported by the National Biomedical Computational Resource (grant No. 2 P41 RR08605) and the National Space Biomedical Research Institute (grant No. IHF00207).

REFERENCES

Aguilar-Bryan, L., C. G. Nichols, S. W. Wechsler, J. P. Clement, A. E. Boyd, G. Gonzales, H. Herrera-Sosa, K. Nguy, J. Bryan, and D. A. Nelson. 1995. Cloning of the beta cell high-affinity sulfonylurea receptor: a regulation of insulin secretion. *Science*. 268:423–426.

Agus, Z. A., E. Kelepouris, I. Dukes, and M. Morad. 1989. Cytosolic magnesium modulates calcium channel activity in mammalian ventricular cells. *Am. J. Physiol.* 256:C425–C455.

Albitz, R., H. Kammermeier, and B. Nilius. 1990. Free energy of ATP-hydrolysis fails to affect ATP-dependent potassium channels in isolated mouse ventricular cells. *J. Mol. Cell. Cardiol.* 22:183–190.

Alekseev, A. E., M. E. Kennedy, B. Navarro, and A. Terzic. 1997. Burst kinetics of co-expressed Kir6.2/SUR1 clones: comparison of recombinant with native ATP-sensitive K^+ channel behavior. *J. Membr. Biol.* 159:161–168.

Ashcroft, F. M., and S. J. Ashcroft. 1990. Properties and functions of ATP-sensitive K-channels. *Cell. Signal.* 2:197–214.

Ashcroft, F. M., and F. M. Gribble. 1998. Correlating structure and function in ATP-sensitive K^+ channels. *Trends Neurosci.* 21:288–294.

Berberian, G., C. Hidalgo, R. DiPolo, and L. Beauge. 1998. ATP stimulation of Na^+/Ca^{2+} exchange in cardiac sarcolemmal vesicles. *Am. J. Physiol.* 274:C724–C733.

Bers, D. M. 2001. Excitation-Contraction Coupling and Cardiac Contractile Force. Kluwer Academic Press, Dortrecht, Boston, MA and London, UK.

Buri, A., and J. A. McGuigan. 1990. Intracellular free magnesium and its regulation, studied in isolated ferret ventricular muscle with ion-selective microelectrodes. *Exp. Physiol.* 75:751–761.

Carmeliet, E. 1999. Cardiac ionic currents and acute ischemia: from channels to arrhythmias. *Physiol. Rev.* 79:917–1017.

Ch'en, F. F. T., R. D. Vaughan-Jones, K. Clarke, and D. Noble. 1998. Modelling myocardial ischaemia and reperfusion. *Prog. Biophys. Mol. Biol.* 69:515–538.

Clement, J. P., K. Kunjilwar, G. Gonzales, M. Schwanstecher, U. Panten, L. Aguilar-Bryan, and J. Bryan. 1997. Association and stoichiometry of K(ATP) channel subunits. *Neuron.* 18:827–838.

Davies, N. W. 1990. Modulation of ATP-sensitive K^+ channels in skeletal muscle by intracellular protons. *Nature.* 343:375–377.

Davies, N. W., N. B. Standen, and P. R. Stanfield. 1991. ATP-dependent potassium channels of muscle cells: their properties, regulation, and possible functions. *J. Bioenerg. Biomembr.* 23:509–535.

Davies, N. W., N. B. Standen, and P. R. Stanfield. 1992. The effect of intracellular pH and ATP-dependent potassium channels of frog skeletal muscle. *J. Physiol.* 445:549–568.

DiPolo, R., and L. Beauge. 1999. Metabolic pathways in the regulation of invertebrate and vertebrate Na^+/Ca^{2+} exchange. *Biochim. Biophys. Acta.* 1422:57–71.

Dunne, M. J., J. J. West, R. J. Abraham, R. H. Edwards, and O. H. Petersen. 1988. The gating of nucleotide-sensitive K^+ channels in insulin-secreting cells can be modulated by changes in the ratio ATP^{4-}/ADP^{-3} and by nonhydrolyzable derivates of both ATP and ADP. *J. Membr. Biol.* 104:165–177.

Eisner, D. A., M. E. Diaz, S. C. O'Neill, and A. W. Trafford. 2004. Physiological and pathological modulation of ryanodine receptor function in cardiac muscle. *Cell Calcium.* 35:583–589.

Fatholahi, M., K. LaNoue, A. Romani, and A. Scarpa. 2000. Relationship between total and free Mg^{2+} during metabolic stimulation of rat cardiac myocytes. *Arch. Biochem. Biophys.* 374:395–401.

Ferrero, J. M., J. J. Saiz, J. M. J. M. Ferrero, and N. V. Thakor. 1996. Simulation of action potentials from metabolic impaired cardiac myocytes: role of ATP-sensitive K^+ current. *Circ. Res.* 79:208–221.

Fridlyand, L. E., N. Tamarina, and L. H. Philipson. 2003. Modeling of Ca^{2+} flux in pancreatic β-cells: role of the plasma membrane and intracellular stores. *Am. J. Physiol.* 285:E138–E154.

Gillis, K. D., W. M. Gee, A. Hammoud, M. L. McDaniel, L. C. Falke, and S. Misler. 1989. Effects of sulfonamides on a metabolic-regulated ATP_i-sensitive K^+ channel in rat pancreatic β-cells. *Am. J. Physiol.* 257:C1119–C1127.

Gribble, F. M., G. Loussouarn, S. J. Tucker, C. Zhao, C. G. Nichols, and F. M. Ashcroft. 2000. A novel method for measurement of submembrane ATP concentration. *J. Biol. Chem.* 29:30046–30049.

Gribble, F. M., S. J. Tucker, and F. M. Ashcroft. 1997. The essential role of the Walker A motifs of SUR1 in K-ATP channel activation by Mg-ADP and diazoxide. *EMBO J.* 16:1145–1152.

Hilgemann, D. W., A. Collins, and S. Matsuoka. 1992. Steady-state and dynamics properties of cardiac sodium-calcium exchange: secondary modulation by cytoplasmic calcium and ATP. *J. Gen. Physiol.* 100:933–961.

Hongo, K., M. Konishi, and S. Kurihara. 1994. Cytoplasmic free Mg^{2+} in rat ventricular myocytes studied with the fluorescent indicator furaptra. *Jpn. J. Physiol.* 44:357–378.

Hopkins, W. F., S. Fatherazi, B. Peter-Riesch, B. E. Corkey, and D. L. Cook. 1992. Two sites for adenine-nucleotide regulation of ATP-sensitive potassium channels in mouse pancreatic β-cells and HIT cells. *J. Membr. Biol.* 129:287–295.

Imredy, J. P., and D. T. Yue. 1994. Mechanism of Ca^{2+}-sensitive inactivation of L-type Ca^{2+} channels. *Neuron.* 12:1301–1318.

Inagaki, N., T. Gonoi, J. P. Clament, N. Namba, J. Inazawa, G. Gonzalez, L. Aguilar-Bryan, S. Seino, and J. Bryan. 1995. Reconstruction of IKATP: an inward rectifier subunit plus the sulfonylurea receptor. *Science.* 270:1166–1169.

Inagaki, N., T. Gonoi, J. P. Clement, C. Z. Wang, L. Aguilar-Bryan, J. Bryan, and S. Seino. 1996. A family of sulfonylurea receptors determines the pharmacological properties of ATP-sensitive K^+ channels. *Neuron.* 16:1011–1017.

Isenberg, G., S. Han, A. Schiefer, and M. F. Wendt-Gallitelli. 1993. Changes in mitochondrial calcium concentration during the cardiac contraction cycle. *Cardiovasc. Res.* 27:1800–1809.

Jafri, M. S., J. J. Rice, and R. L. Winslow. 1998. Cardiac Ca^{2+} dynamics: the roles of ryanodine receptor adaptation and sarcoplasmic reticulum load. *Biophys. J.* 74:1149–1168.

Karschin, A., J. Brockhaus, and K. Ballanyi. 1998. K_{ATP} channel formation by the sulphonylurea receptors SUR1 with Kir6.2 subunits in rat dorsal vagal neurons in situ. *J. Physiol.* 509:339–346.

Kleber, A. G. 1983. Resting membrane potential, extracellular potassium activity, and intracellular sodium activity during acute global ischemia in isolated perfused guinea pig hearts. *Circ. Res.* 52:442–450.

Laver, D. R., T. M. Baynes, and A. F. Dulhunty. 1997. Magnesium inhibition of ryanodine-receptor calcium channels: evidence for two independent mechanisms. *J. Membr. Biol.* 156:213–229.

Lederer, W. J., and C. G. Nichols. 1989. Nucleotide modulation of the activity of rat heart ATP-sensitive K^+ channels in isolated membrane patches. *J. Physiol.* 419:193–211.

Lorenz, E., A. E. Alekseev, G. B. Krapivinsky, A. J. Carrasco, D. E. Clapham, and A. Terzic. 1998. Evidence for direct physical association between a K+ channel (Kir6.2) and an ATP-binding cassette protein (SUR1) which affects cellular distribution and kinetic behavior of an ATP-sensitive K+ channel. *Mol. Cell. Biol.* 18:1652–1659.

Matsuoka, S., N. Sarai, S. Kuratomi, K. Ono, and A. Noma. 2003. Role of individual ionic current systems in ventricular cells hypothesized by a model study. *Jpn. J. Physiol.* 53:105–123.

Michailova, A. P., and A. D. McCulloch. 2001. Model study of ATP and ADP buffering, transport of Ca^{2+} and Mg^{2+}, and regulation of ion pumps in ventricular myocyte. *Biophys. J.* 81:614–629.

Michailova, A. P., M. E. Thomas, and A. D. McCulloch. 2004a. Cytosolic magnesium and adenine-nucleotide phosphates modulate cardiac excitation-contraction coupling. *Biophys. J.* 86:287a (Abstr.).

Michailova, A., M. E. Belik, and A. McCulloch. 2004b. Effects of magnesium on cardiac excitation-contraction coupling. *J. Am. Coll. Nutr.* 23:514S–517S.

Murphy, E. 2000. Mysteries of magnesium homeostasis. *Circ. Res.* 86:245–248.

Nichols, C. G., and W. J. Lederer. 1991. Adenosine triphosphate-sensitive potassium channels in the cardiovascular system. *Am. J. Physiol.* 261: H1675–H1686.

Nichols, C. G., C. Ripoll, and W. J. Lederer. 1991a. ATP-sensitive potassium channel modulation of the guinea pig ventricular action potential and contraction. *Circ. Res.* 68:280–287.

Nichols, C. G., W. J. Lederer, and M. B. Cannel. 1991b. ATP dependence of K_{ATP} channel kinetics in isolated membrane patches from rat ventricle. *Biophys. J.* 60:1164–1177.

Nichols, C. G., S. L. Shyng, A. Nestorowicz, B. Glaser, J. P. Clement 4th, G. Gonzalez, L. Aguilar-Bryan, M. A. Permutt, and J. Bryan. 1996c. Adenosine diphosphate as an intracellular regulator of insulin secretion. *Science.* 272:1785–1787.

Noma, A. 1983. ATP-regulated K^+ channels in cardiac muscle. *Nature.* 305:147–148.

Noma, A., and T. Shibasaki. 1985. Membrane current through adenosine-triphosphate-regulated potassium channels in guinea-pig ventricular cells. *J. Physiol.* 363:463–480.

O'Rourke, B., P. H. Backx, and E. Marban. 1992. Phosphorylation-independent modulation of L-type calcium channels by magnesium-nucleotide complexes. *Science.* 257:245–248.

Pelzer, S., C. C. La, and K. L. Pelzer. 2001. Phosphorylation-dependent modulation of cardiac calcium current by intracellular free magnesium. *Am. J. Physiol.* 281:H1532–H1544.

Proks, P., and F. M. Ashcroft. 1997. Phentolamine block of KATP channels is mediated by Kir6.2. *Proc. Natl. Acad. Sci. USA.* 94:11716–11720.

Ravens, U., E. Wettwer, and O. Hala. 2004. Pharmacological modulation of ion channels and transporters. *Cell Calcium.* 35:575–582.

Ribalet, B., S. A. John, and J. N. Weiss. 2003. Molecular basis for Kir6.2 channel inhibition by adenine nucleotides. *Biophys. J.* 84:266–276.

Rice, J., S. Jafri, and R. Winslow. 1999. Modeling gain and gradedness of Ca^{2+} release in the functional unit of the cardiac diadic space. *Biophys. J.* 77:1871–1884.

Rodriguez, B., J. M. Ferrero, Jr., and B. Trenor. 2002. Mechanistic investigation of extracellular K^+ accumulation during acute myocardial ischemia: a simulation study. *Am. J. Physiol.* 283:H490–H500.

Romani, A., and A. Scarpa. 1990. Hormonal control of Mg^{2+} in the heart. *Nature.* 346:841–844.

Romani, A., and A. Scarpa. 2002. Regulation of cellular magnesium. *Front. Biosci.* 5:720–734.

Sakura, H., C. Ammala, P. A. Smith, F. M. Gribble, and F. M. Ashcroft. 1995. Cloning and functional expression of the cDNA encoding a novel ATP-sensitive potassium channel subunit expressed in pancreatic beta-cells, brain, heart and skeletal muscle. *FEBS Lett.* 377:338–344.

Shaw, R. M., and Y. Rudy. 1994. Electrophysiological changes of ventricular tissue under ischemic conditions: a simulation study. *Comput. Cardiol.* 16:641–644.

Shaw, R. M., and Y. Rudy. 1997. Electrophysiologic effects of acute myocardial ischaemia: a theoretical study of altered cell excitability and action potential duration. *Cardiovasc. Res.* 35:256–272.

Shyng, S. L., and C. G. Nichols. 1997. Octameric stoichiometry of the K_{ATP} channel complex. *J. Gen. Physiol.* 110:655–664.

Spruce, A. E., N. B. Standen, and P. R. Stanfield. 1987. Studies of the unitary properties of adenosine-5′-triphosphate-regulated potassium channels of frog skeletal muscle. *J. Physiol.* 382:213–236.

Tamargo, J., R. Caballero, R. Gomez, C. Valenzuela, and E. Delpon. 2004. Pharmacology of cardiac potassium channels. *Cardiovasc. Res.* 62:9–33.

Trapp, S., S. J. Tucker, and F. M. Ashcroft. 1997. Activation and inhibition of K-ATP currents by guanine nucleotides is mediated by different channel subunits. *Proc. Natl. Acad. Sci. USA.* 94:8872–8877.

Tucker, S. J., F. M. Gribble, C. Zhao, S. Trapp, and F. M. Ashcroft. 1997. Truncation of Kir6.2 produces ATP-sensitive K+ channels in the absence of the sulphonylurea receptor. *Nature.* 387:179–183.

Valdivia, H. H., J. H. Kaplan, G. C. R. Ellis-Davies, and W. J. Lederer. 1995. Rapid adaptation of cardiac ryanodine receptors: modulation by Mg^{2+} and phosphorylation. *Science.* 267:1997–2000.

Wang, M., M. Tashiro, and J. Berlin. 2003. Regulation of L-type calcium current by intracellular magnesium in rat cardiac myocytes. *J. Physiol.* 555:383–396.

Wei, S., J. F. Quigley, S. U. Hanlon, B. O'Rourke, and M. C. P. Haigney. 2002. Cytosolic free magnesium modulates Na/Ca exchange currents in pig myocytes. *Cardiovasc. Res.* 53:334–340.

Weiss, J. N., N. Venkatesh, and S. T. Lamp. 1992. ATP-sensitive K^+ channels and cellular K^+ loss in hypoxic and ischaemic mammalian ventricle. *J. Physiol.* 447:649–673.

Winslow, R. L., J. Rice, S. Jafri, E. Marban, and B. O'Rourke. 1999. Mechanisms of altered excitation-contraction coupling in canine tachycardia-induced heart failure. II. Model studies. *Circ. Res.* 84:571–586.

Ueda, K., N. Inagaki, and S. Seino. 1997. MgADP Antagonism to Mg^{2+}-independent ATP binding of the sulfonylurea receptor SUR1. *J. Biol. Chem.* 272:22983–22986.

Xu, L., G. Mann, and G. Meissner. 1996. Regulation of cardiac Ca^{2+} release channel (ryanodine receptor) by Ca^{2+}, H^+, Mg^{2+}, and adenine nucleotides under normal and simulated ischemic conditions. *Circ. Res.* 79:1100–1109.

Yamaoka, K., T. Yuki, K. Kawase, M. Munemori, and I. Seyama. 2002. Temperature-sensitive intracellular Mg^{2+} block of L-type Ca^{2+} channels in cardiac myocytes. *Am. J. Physiol.* 282:H1092–H1101.

Yazawa, K., A. Kameyama, K. Yasui, J.-M. Li, and M. Kameyama. 1997. ATP regulates cardiac Ca^{2+} channel activity via a mechanism independent of protein phosphorylation. *Pflugers Arch.* 433:557–562.

Zahradnikova, A., M. Dura, I. Gyorke, A. L. Escobar, I. Zahradnik, and S. Gyorke. 2003. Regulation of dynamic behavior of cardiac ryanodine receptor by Mg^{2+} under simulated physiological conditions. *Am. J. Physiol.* 285:C1059–C1070.